

Damping Vibrations in  
a Dual-Beam Flexible Robotic Arm

MEEN 485:  
University Undergraduate Fellows Thesis

Submitted by:  
Russell Read

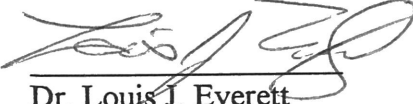
Texas A&M University  
Department of Mechanical Engineering  
April 14, 1994

DAMPING VIBRATIONS IN  
A DUAL-BEAM FLEXIBLE ROBOTIC ARM

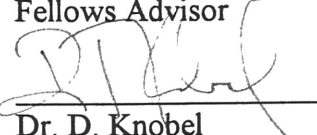
by  
Russell Read  
University Undergraduate Fellow, 1993-1994

Texas A&M University  
Department of Mechanical Engineering

APPROVED



Dr. Louis J. Everett  
Fellows Advisor



Dr. D. Knobel  
Honors Director

## TABLE OF CONTENTS

CHAPTER		Page
I	INTRODUCTION .....	1
	Introduction.....	1
	Problem Description and History .....	1
	Summary .....	3
II	DEVELOPMENT OF MODEL .....	5
	Simplifications and Assumptions .....	5
	Equations of Motion.....	8
	Kinematics.....	12
III	ACTUATOR METHOD .....	16
	Theory.....	16
	Simulation .....	18
	Results .....	20
	Discussion .....	20
IV	SPRING-DAMPER METHOD.....	22
	Theory.....	22
	Simulation .....	24
	Results .....	26
	Discussion .....	31
V	CONCLUSION .....	33
	Summary .....	33
	Recommendations for Future Study .....	33
	REFERENCES .....	35
	APPENDIX A .....	36
	Part 1 .....	36
	Part 2 .....	38
	Part 3 .....	40
	Part 4 .....	42
	APPENDIX B.....	44

## LIST OF FIGURES

Figure		Page
1.	Typical robotic arm configuration and modeling .....	2
2.	Comparison of single-beam link to dual-beam link .....	3
3.	Schematic of stopped, single-link, dual-beam system .....	5
4.	Model of the complete system .....	6
5.	Schematic showing pseudolink .....	6
6.	Free-body diagram of Beam 1 .....	8
7.	Free-body diagram of Beam 2 .....	10
8.	Free-body diagram of Endmass .....	11
9.	Free-body diagram of Pins B and C .....	12
10.	Kinematics set-up for $\beta$ and $\phi$ .....	13
11.	Parallel beam configuration .....	16
12.	In-drawn configuration.....	17
13.	Pressed-out beam configuration.....	18
14.	Force provided by actuator.....	19
15.	Diagram of system after base motion stops .....	22
16.	Diagram of system with beams past equilibrium.....	23
17.	Point of passing equilibrium.....	23
18.	Displacement from equilibrium given initial $\theta$ displacement.....	25
19.	Stable system displacement of endmass .....	28
20.	Unstable system displacement of endmass.....	29
21.	Endmass settling time as a function of mass.....	29
22.	Endmass settling time as a function of $d_1$ .....	30
23.	Endmass settling time as a function of configuration.....	30

## ABSTRACT

Robots have contributed a great deal to manufacturing industry, increasing both productivity and quality. However, they often achieve accuracy for quality by adding mass to their links, increasing weight and power required for operation. Once the mass is removed, though, vibrations in the flexible system make accurate work very difficult.

Some study has been done on active controllers for flexible links in order to damp their oscillation. The purpose of this investigation is to develop a passive control scheme which takes advantage of a new configuration of the flexible arm. This configuration has two parallel beams in every link as opposed to the one found in other investigations. This investigation models the first link of a flexible planar manipulator.

Two methods of removing the oscillations were modeled. The first involved actively controlling the distance between the ends of the two beams in the first link. The hypothesis behind this method was to change the center of rotation of the endmass to remove energy. This method was not successful. The next involved placing a spring-damper system between each beam and the endmass and allowing the dampers to remove energy from the system. This method was successful, having settling times ranging from 0.75 s to 9.75 s.

## CHAPTER 1

### INTRODUCTION

#### INTRODUCTION

One area of engineering which has been the subject of some study is robotics. This field received a great deal of interest in its infancy due to the promise it offered as an enhancement for manufacturing. And it delivered. From cars to clothes and from machines to milk, robotics have enhanced manufacturing and processing both in terms of speed and quality. However, eventually a point was reached that further improvements would become very costly. At this point, industry lost some of their interest, and with it went a good deal of support.

However, technology is constantly advancing, and with advancement comes new opportunities. With the new technology now available in materials and actuators, the field of robotics has the opportunity for many improvements. One of these possible improvements involves the dynamics of the manipulator itself.

#### PROBLEM DESCRIPTION AND HISTORY

Generally, the movement of a robotic manipulator is caused by an actuator, typically an electrical motor, located at one end of each manipulator "link." When this actuator is activated, it causes the link to move. However, due to its inertia and compliance, the other end of the link will "lag" behind the actuator end in its motion. When the actuator stops, the other end can continue moving. This causes an oscillation of the end of the link, sending vibrations through the structure. These vibrations make it difficult to perform delicate tasks with any degree of accuracy.

One way to solve this problem is by making the links stiffer and more rigid. Typically, this is done by adding material to the links. Eventually, enough mass can be added to make them thick and strong enough to be modeled as rigid. However, this is not desirable. As links become bulkier, the actuators required to move them become larger as well. If the size of the links were

to be reduced, then smaller and simpler actuators could be used to move them, reducing cost and energy consumption and increasing speed. To implement these smaller, inherently flexible, links, it is necessary to have some method of controlling their oscillatory motion.

Much research has been done concerning flexible manipulators due to the many benefits of a lighter system. Nathan and Singh [1] used a nonlinear ultimate boundedness controller with a feedback stabilizer to control the arm about the equilibrium state. Jankowski and van Brussel [2] used an inverse-dynamics method to develop a discrete time control of a flexible joint arm. Another method which has been used relatively successfully is a variable structure scheme, where the control algorithm changes based on the condition of the end of the arm [3, 4, 5]. Finally, efforts have also been made to develop a "passive" controller, which works with a finite gain, providing the link is adequately stiff [6].

Although most of the systems above use a single link in order to simplify the problem, most robotic arms are composed of multiple links, arranged as shown in Figure 1a. However, the single link assumption will work for multiple links if a specific mass and mass moment of inertia are given to the endmass. This mass and mass moment of inertia can be found such that they accurately represent the links which would be located beyond the link being modeled (see Figure 1b).

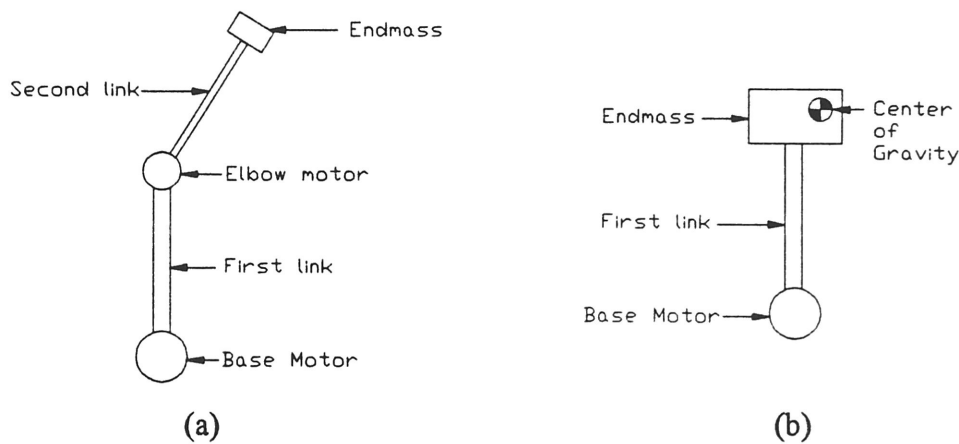


FIGURE 1: a) Typical robotic arm configuration and b) Modeling for the first link

## SUMMARY

This approach to the problem of damping the vibrations in the flexible arm was slightly different than the ones presented above. First, this controller was to be passive. This means that little or no feedback is to be required for operation. Second, this approach will take advantage of a different structure than that used in the instances above. Like the other systems, this model will be horizontally planar and a single link. However, this single link will be composed of two beams as opposed to the single beam represented in Figure 1a and 1b (see Figure 2). Although this system will weigh more than a link of a single beam, the weight will still be significantly below that of a stiff-link system.

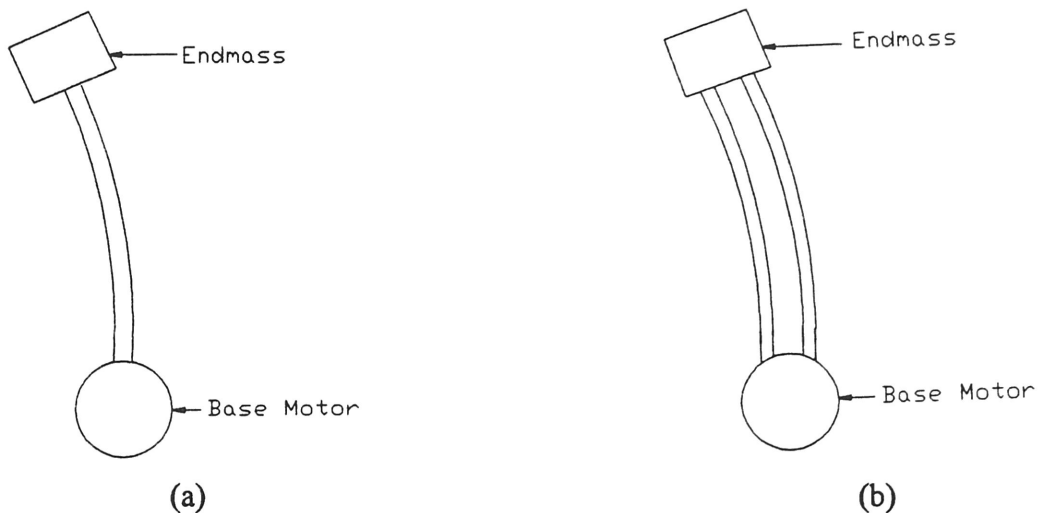


FIGURE 2: Comparison of a) Single-beam link to b) Dual-beam link

There are two advantages to having two beams. Each of these advantages is the basis for a method of removing the oscillation from the system. The first method actively changes the distance between the ends of the two beams as compared to the distance between the two beams at the base. This changes the geometry of the system and thus alters its dynamics. The second method uses differences in relative motion between the end of each beam and the endmass to remove energy from the system by means of linear dampers. In addition, springs are used to



change the natural length of the distance between the ends of the two beams so that different geometries can be explored as well.

In order to determine the better of these methods, both were simulated using the Advanced Continuous Simulation Language (ACSL). In addition to simulating the two different methods, several parameters were also varied in an effort to determine some relationship between the parameters and the damping of the vibration.

Before beginning to simulate the system, a model must first be developed. This will be done in Chapter II. In Chapter III, the actuator method will be discussed, including its theory and the results of the simulation. The damper-spring method, with its theory and results, will be the topic of Chapter IV. Finally, Chapter V will summarize the results and recommend future study.

## CHAPTER II

### DEVELOPMENT OF MODEL

#### SIMPLIFICATIONS AND ASSUMPTIONS

Several simplifications were made to the system in order to show the general behavior of each method. First, the simplification was made that the first link (i.e. the link connected to the base motor) would be the one modeled, allowing extra links to be modeled by the mass and mass moment of inertia of the endmass. Furthermore, the oscillation will be damped after the arm has stopped, allowing the base joint to be modeled as rigid. These simplifications are shown schematically in Figure 3. The extensions from the endmass represent the fact that the distance between the ends of the beams is not fixed, but is variable. This schematic leads directly to the model of the system as shown in Figure 4.

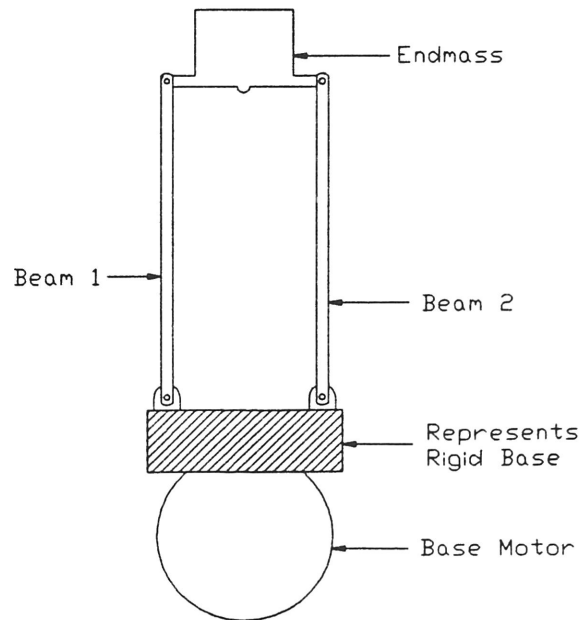


FIGURE 3: Schematic of the stopped, single-link, dual beam system

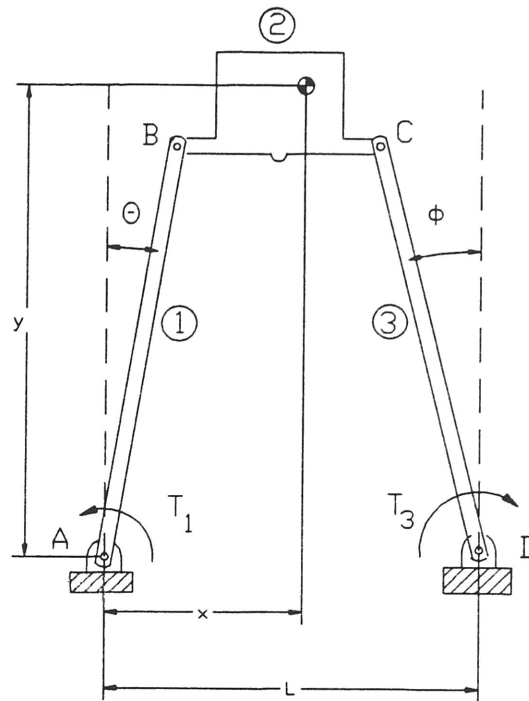


FIGURE 4: Model of Complete System

Some assumptions were then made. One assumption which was made was that any deflection in the beams will be small, which allows the assumption of small angles. Also, the deflection of each beam was modeled as a pseudolink, as done by Mahmood and Walcott [4]. This means that only the deflection of the tips of the beams are taken into account, as seen in Figure 5. This assumption allows the connection between the beams and the base to be modeled as pinned.

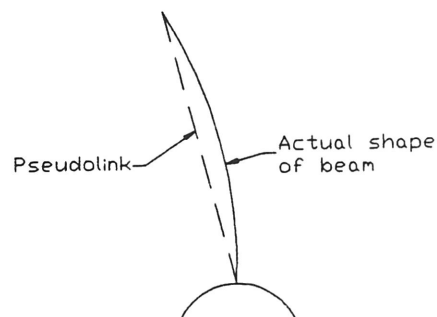


FIGURE 5: Schematic showing pseudolink

The pseudolink assumption can be validated by using the beam theory. According to this theory, the displacement of a beam due to a force applied perpendicularly to the end of the beam at the end of the beam is

$$\delta = \frac{PL^3}{3EI} \quad (1)$$

where  $\delta$  is the linear deflection of the end of the beam  
 $P$  is the applied force at the end of the beam  
 $L$  is the length of the beam  
 $E$  is Young's modulus for the material of the beam  
 $I$  is the second moment of area for the beam

We also know that, for a force that is perpendicular to the beam,

$$T = PL \quad (2)$$

where  $T$  is the restoring torque at the base

In addition, for small angles, the deflection can also be described as

$$\delta = L \cdot \sin\theta \quad (3)$$

where  $\theta$  is the difference in direction between the vector from the base to the equilibrium point and the vector from the base to the final point

and, by the small angle assumption,

$$\sin\theta \approx \theta \quad (4)$$

Substituting Equation (4) into Equation (3), then substituting (3) and (2) into (1), and finally with a little algebraic manipulation, we get the equation

$$T = \frac{3EI}{L} \cdot \theta \quad (5)$$

Here,  $E$ ,  $I$ , and  $L$  are all constants, so the  $\frac{3EI}{L}$  term can be combined into a single constant  $k$  to give the equation

$$T = k\theta \quad (6)$$

where  $k$  is a stiffness factor for the beam

## EQUATIONS OF MOTION

Once these assumptions are made, the system as shown in Figure 4 can be divided into components. For each of these components, a free-body diagram can be drawn which shows the outside forces and torques. By summing these forces and using dynamics, differential equations can be developed which begin to describe the system.

The first component modeled is Pseudobeam 1, whose angular deflection from directly forward is described by the variable  $\theta$ . In this case, directly forward is the direction that the beam would be pointing at equilibrium if the beams were parallel. This component is shown schematically in Figure 6.

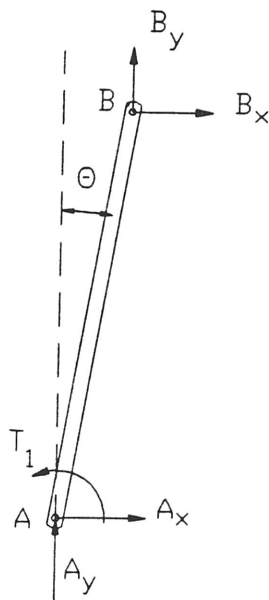


FIGURE 6: Free-body diagram of Beam 1

By summing moments about the base point A, we get

$$\sum M_A = -T_1 + B_x \ell_1 \cos(\theta) - B_y \ell_1 \sin(\theta) = I_1 \ddot{\theta} \quad (7)$$

where  $T_1$  is the restoring torque at the base at point A  
 $B_x$  and  $B_y$  are the forces acting on Pseudobeam 1 at point B  
 $\ell_1$  is the length of Beam 1  
 $I_1$  is the mass moment of inertia of Beam 1 about point A

Modeling the torque as a torsional spring as described in Equation 6, we get

$$T_1 = k_1 \theta \quad (8)$$

and by representing the beam as a thin plate on an edge,  $I_1$  becomes

$$I_1 = \frac{1}{3} m_1 \ell_1^2 \quad (9)$$

where  $m_1$  is the mass of Beam 1

which simplifies Equation 6 to

$$-k_1 \theta + B_x \ell_1 \cos \theta - B_y \ell_1 \sin \theta = \frac{1}{3} m_1 \ell_1^2 \ddot{\theta} \quad (10)$$

By the same methods, due to their assumed symmetry, Pseudobeam 2, shown below in Figure 7, can be modeled by Equation 11.

$$-k_3 \phi + C_x \ell_3 \cos \phi - C_y \ell_3 \sin \phi = \frac{1}{3} m_3 \ell_3^2 \ddot{\phi} \quad (11)$$

where  $\phi$  is the angular deflection of Beam 2  
 $C_x$  and  $C_y$  are the forces acting on Beam 2 at point C  
 $\ell_3$  is the length of Beam 2  
 $m_3$  is the mass of Beam 2

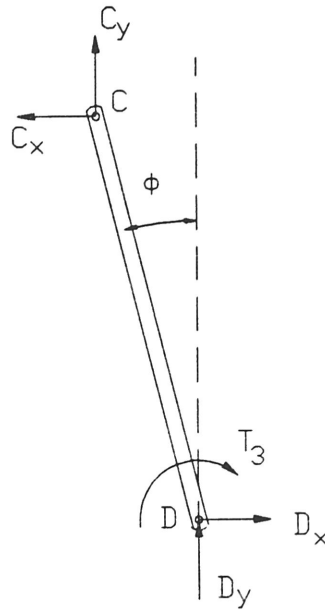


FIGURE 7: Free-body diagram of Beam 2

Figure 8 contains the model of the mass at the end of the link. As described before, this endmass includes everything outward from the end of the link, including additional joints, additional links, end manipulators, and any objects being carried. For simplicity without compromising versatility, the mass is represented by a lump mass with a given center of gravity and mass moment of inertia. For the purposes of this model, both  $l_{2A}$  and  $l_{2B}$  are assumed to have variable lengths. It is by changing the sum of these two lengths that the geometry of the system is controlled.

There are three equations of motion within this diagram. First, summing forces in the x-direction,

$$C_{2x} - B_{2x} = m_2 \ddot{x} \quad (12)$$

where  $m_2$  is the mass of the endmass  
 $x$  is the displacement from base point A to the center of gravity  
of the endmass in the x-direction

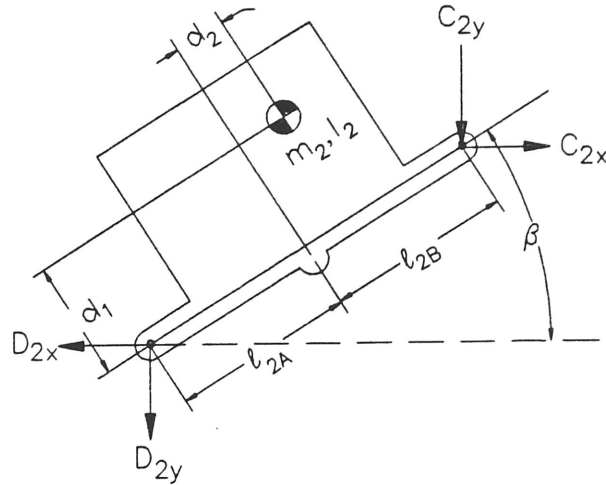


FIGURE 8: Free-body diagram of Endmass

Next, summing forces in the y-direction

$$-B_{2y} - C_{2y} = m_2 \ddot{y} \quad (13)$$

where  $y$  is the vertical displacement from base point A to the center of gravity of the endmass

Finally, summing moments about the center of gravity

$$\begin{aligned} -B_{2x}(\ell_{2A} \sin \beta + d_1 \cos \beta + d_2 \sin \beta) + B_{2y}(\ell_{2A} \cos \beta - d_1 \sin \beta + d_2 \cos \beta) \\ - C_{2x}(-\ell_{2B} \sin \beta + d_1 \cos \beta + d_2 \sin \beta) - C_{2y}(\ell_{2B} \cos \beta + d_1 \sin \beta + d_2 \cos \beta) = I_2 \ddot{\beta} \end{aligned} \quad (14)$$

where  $I_2$  is the mass moment of inertia of the endmass

The final free-body diagrams to be drawn are for the pins at B and C, as shown in Figure 9. Because these pins are assumed to be essentially massless, the summation of forces in the x- and y- directions must equal zero for each pin, resulting in the Equations 15-18.

$$B_x = B_{2x} \quad (15)$$

$$B_y = B_{2y} \quad (16)$$

$$C_x = C_{2x} \quad (17)$$

$$C_y = C_{2y} \quad (18)$$



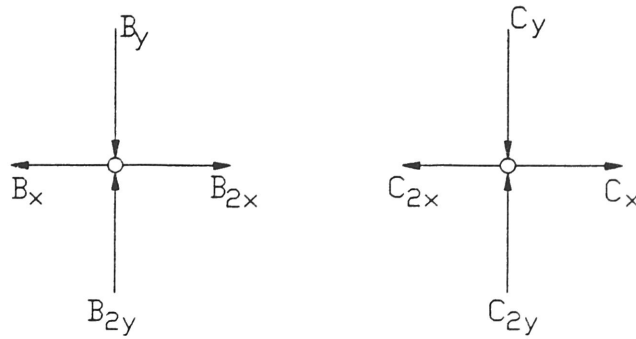


FIGURE 9: Free-body diagram of pins B and C

## KINEMATICS

Despite the fact that all the components have been modeled, the system is still not completely described, as proven by the fact that there are still more unknowns than equations. Now, the interaction of the components with each other must be described using kinematics. To place the center of gravity of the endmass with respect to the fixed point at A in the x-direction, Figure 2 is used to produce the equation

$$x = \ell_1 \sin \theta + \ell_{2A} \cos \beta - d_1 \sin \beta + d_2 \cos \beta \quad (19)$$

Taking the derivative with respect to time involves using the chain rule with  $\theta$ ,  $\ell_{2A}$ , and  $\beta$  as the intermediate variables. Doing so once gives

$$\dot{x} = \ell_1 \dot{\theta} \cos \theta + \dot{\ell}_{2A} \cos \beta - \dot{\beta} (\ell_{2A} \sin \beta + d_1 \cos \beta + d_2 \sin \beta) \quad (20)$$

Doing so a second time gives

$$\begin{aligned} \ddot{x} = & \ell_1 \ddot{\theta} \cos \theta - \ell_1 \dot{\theta}^2 \sin \theta + \ddot{\ell}_{2A} \cos \beta - 2 \dot{\ell}_{2A} \dot{\beta} \sin \beta - \ddot{\beta} (\ell_{2A} \sin \beta + d_1 \cos \beta + d_2 \sin \beta) \\ & - \dot{\beta}^2 (\ell_{2A} \cos \beta - d_1 \sin \beta + d_2 \cos \beta) \end{aligned} \quad (21)$$

Placing the center of gravity of the endmass with respect to the fixed point at A in the y-direction produces the equation

$$y = -\ell_1 \cos\theta + \ell_{2A} \sin\beta + d_1 \cos\beta + d_2 \sin\beta \quad (22)$$

The first derivative of this equation with respect to time gives

$$\dot{y} = -\ell_1 \dot{\theta} \sin\theta + \dot{\ell}_{2A} \sin\beta + \dot{\beta}(\ell_{2A} \cos\beta - d_1 \cos\beta + d_2 \cos\beta) \quad (23)$$

The second differentiation of this equation gives

$$\begin{aligned} \ddot{y} = & -\ell_1 \ddot{\theta} \sin\theta - \ell_1 \dot{\theta}^2 + \ddot{\ell}_{2A} \sin\beta + 2\dot{\ell}_{2A} \dot{\beta} \cos\beta + \ddot{\beta}(\ell_{2A} \cos\beta - d_1 \sin\beta + d_2 \cos\beta) \\ & - \ddot{\beta}(\ell_{2A} \sin\beta + d_1 \cos\beta + d_2 \sin\beta) \end{aligned} \quad (24)$$

Next, the angle  $\beta$  and its derivatives will be found. Because the angles  $\theta$  and  $\phi$  are defined from the equilibrium positions of the two beams when they are parallel, the assumption can be made that the line connecting the base points of the two beams is perpendicular to the  $0^\circ$  angles of  $\theta$  and  $\phi$ . From this, the assumption can be made that the distance in the y-direction to a point from either of the base points will be the same (see Figure 10).

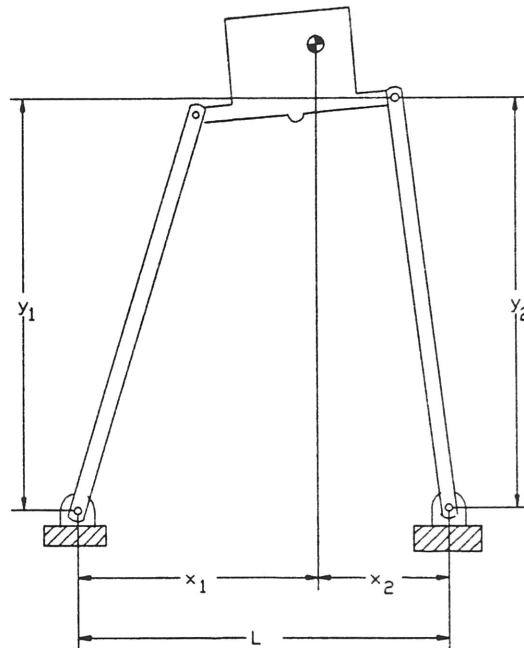


FIGURE 10

Thus we can set up the equation:

$$Y_1 = Y_2$$

$$\ell_1 \cos\theta + (\ell_{2A} + \ell_{2B}) \sin\beta = \ell_3 \cos\phi \quad (25)$$

and get the following equations

$$\beta = \sin^{-1} \left[ \frac{\ell_3 \cos\phi - \ell_1 \cos\theta}{\ell_{2A} + \ell_{2B}} \right] \quad (26)$$

$$\dot{\beta} = \frac{1}{(\ell_{2A} + \ell_{2B}) \cos\beta} \left[ \ell_1 \dot{\theta} \sin\theta - \ell_3 \dot{\phi} \sin\phi - (\dot{\ell}_{2A} + \dot{\ell}_{2B}) \sin\beta \right] \quad (27)$$

$$\ddot{\beta} = \frac{1}{(\ell_{2A} + \ell_{2B}) \cos\beta} \left[ \begin{aligned} &\ell_1 \ddot{\theta} \sin\theta + \ell_1 \dot{\theta}^2 \cos\theta + (\ell_{2A} + \ell_{2B}) \dot{\beta}^2 \sin\beta - 2(\dot{\ell}_{2A} + \dot{\ell}_{2B}) \dot{\beta} \cos\beta \\ &- (\ddot{\ell}_{2A} + \ddot{\ell}_{2B}) \sin\beta - \ell_3 \ddot{\phi} \sin\phi - \ell_3 \dot{\phi}^2 \cos\phi \end{aligned} \right] \quad (28)$$

Likewise, we can assume that the sum of the x-direction distances will be equal to the distance between the two bases (see Figure 10). This produces the equation

$$x_1 + x_2 = L$$

$$\ell_1 \sin\theta + (\ell_{2A} + \ell_{2B}) \cos\beta + \ell_3 \sin\phi = L \quad (29)$$

which is used to produce

$$\phi = \sin^{-1} \left[ \frac{L - \ell_1 \sin\theta - (\ell_{2A} + \ell_{2B}) \cos\beta}{\ell_3} \right] \quad (30)$$

$$\dot{\phi} = -\frac{1}{\ell_3 \cos\phi} \left[ \ell_1 \dot{\theta} \cos\theta - (\ell_{2A} + \ell_{2B}) \dot{\beta} \sin\beta + (\dot{\ell}_{2A} + \dot{\ell}_{2B}) \cos\beta \right] \quad (31)$$

$$\ddot{\phi} = \frac{1}{\ell_3 \cos\phi} \left[ \begin{aligned} &-\ell_1 \ddot{\theta} \cos\theta + \ell_1 \dot{\theta}^2 \sin\theta + (\ell_{2A} + \ell_{2B}) \dot{\beta} \sin\beta + (\ell_{2A} + \ell_{2B}) \dot{\beta}^2 \cos\beta \\ &+ 2(\dot{\ell}_{2A} + \dot{\ell}_{2B}) \dot{\beta} \sin\beta - (\ddot{\ell}_{2A} + \ddot{\ell}_{2B}) \cos\beta + \ell_3 \dot{\phi}^2 \sin\phi \end{aligned} \right] \quad (32)$$

These equations are combined to give a set of differential equations which can be used to completely describe the system, if given the correct number of inputs. The number of inputs will

depend on the number of degrees of freedom allowed, which differs for the two damping methods used, and will therefore be discussed in the respective chapters.

For the simulations, numbers had to be found to use for each of these variables. The numbers used represented the base link of a flexible two-link planar arm which has been built at Texas A&M University. From [7], values were found to use for the lengths and masses of the beams and the base length. An approximate value was found experimentally for the stiffness of the beams. This stiffness involved measuring the deflections resulting from the application of known forces perpendicular to the end of the beam. The deflections were then converted to angles by using the formula

$$\psi = \sin^{-1}\left(\frac{\delta}{\ell}\right) \quad (33)$$

where  $\psi$  is the angular deflection  
 $\delta$  is the linear deflection of end of the beam  
 $\ell$  is the length from the pinned end of the beam to the point of force application

Then the forces applied to the end of the beam were converted to torques using the formula

$$T = F\ell \quad (34)$$

where  $F$  is the force applied  
 $T$  is the resulting torque

The stiffness was then determined to be the slope of the best straight line curve fit to the plot of the torque as a function of the angular displacement.

The remaining variables, including mass, mass moment of inertia, and location of the center of gravity of the endmass, and the offset of the equilibrium angle of the beams from parallel were not fixed. This was to allow some flexibility in the simulations to test the reaction of the system to different situations.

## CHAPTER III

## ACTUATOR METHOD

## THEORY

The first method considered to damp the vibration of the flexible arm involved controlling the distance between the endmass and each of the beams in the link. This method was based on the differences in motion resulting from different configurations of the beams.

Shown in Figure 11 is a schematic of the system with the beams of the link parallel. With the beams in this configuration, motion of the endmass is purely translational for small deflections. This can be seen by drawing the velocity vectors at the ends of the beams. If the distance between the ends of the beam is kept the same as the base distance, then the velocity vectors, which are perpendicular to the end of the beams, will always be parallel. Since the ends of the beams are directly connected to the endmass, these connection points on the endmass will have equal velocity vectors at corresponding points. These velocity vectors place the instantaneous center of rotation for the endmass at infinity, indicating translational motion.

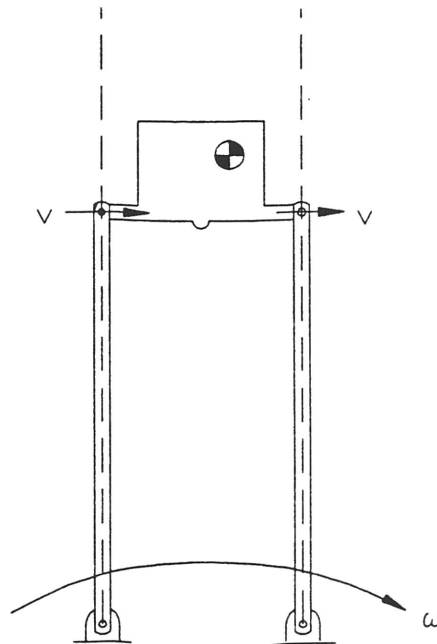


FIGURE 11: Parallel beam configuration

However, if the beams are drawn inwards such that the distance between the tips is less than the base distance (see Figure 12), the situation changes. Again, the velocity vectors are perpendicular to the end of the beams, but now they are no longer parallel. These vectors give a center of rotation for the endmass at a finite distance beyond the endmass, meaning that the endmass has some element of rotation.

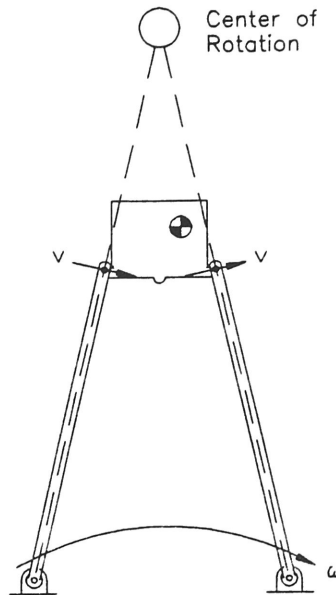


FIGURE 12: In-drawn beam configuration

Likewise, if the distance between the ends is greater than the base distance, or the beams are pressed outward, the situation is different. Again the direction of the velocity vectors indicate a center of rotation for the endmass at a finite distance from the base, but this time, the center of rotation is back behind the base. This gives rotation of the endmass in the opposite direction from in-drawn beams for the same rotational velocity direction (see Figure 13).

The hypothesis was that changing the rotation of the endmass would remove energy from the system. This was to be done by changing the lengths of the actuators  $\ell_{2A}$  and  $\ell_{2B}$  to give the in-drawn and pressed-out configurations. This change in length was to be done in a variety of patterns, including sinusoidally, instantaneously, etc., in order to determine the most effective for removing energy from the system, and thus damping the oscillation.

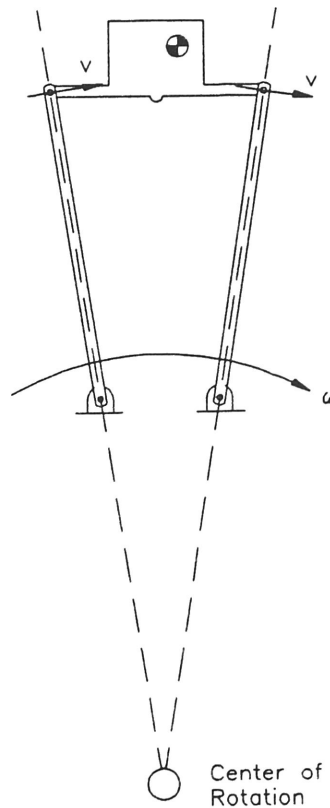


FIGURE 13: Pressed-out beam configuration

## SIMULATION

Before simulating the motion of the system, the number of degrees of freedom had to be determined to fix the number of state variables required. If the lengths of both  $\ell_{2A}$  and  $\ell_{2B}$  are known, the system is a simple four-bar system, giving it one degree-of-freedom. However, an actuator can only provide a finite amount of force, and becomes saturated past that point. For a saturated actuator, the applied force is known, and the length can be derived from that. For each saturated actuator, one more degree-of-freedom is added. This gives a maximum of three degrees-of-freedom.

Given a different number of degrees-of-freedom, different variables are known. Therefore, four different means of obtaining the information necessary for each time step had to be devised. From these, two numerical integrations could be performed on an acceleration value for each degree-of-freedom to give velocity and position information for the initial conditions for the next time step.

For one degree-of-freedom, the initial conditions were  $\theta, \dot{\theta}, l_{2A}, l_{2B}, \dot{l}_{2A}, \dot{l}_{2B}, \ddot{l}_{2A}$ , and  $\ddot{l}_{2B}$ . The other variables could be found using a scheme as shown in Appendix A, Part 1. The ultimate goal was to find  $\ddot{\theta}$ , which could be integrated to give  $\dot{\theta}$  and  $\theta$ . From there, a new set of values were calculated for the other variables, and the process began again.

For a two degree-of-freedom system, the values involving either  $l_{2A}$  and  $l_{2B}$  were removed, depending on which was saturated. This was replaced by values for  $\phi$  and  $\dot{\phi}$  which were found by integrating the value for  $\ddot{\phi}$  found in the previous time step. Also, the length of the actuator can be approximated with the following graph:

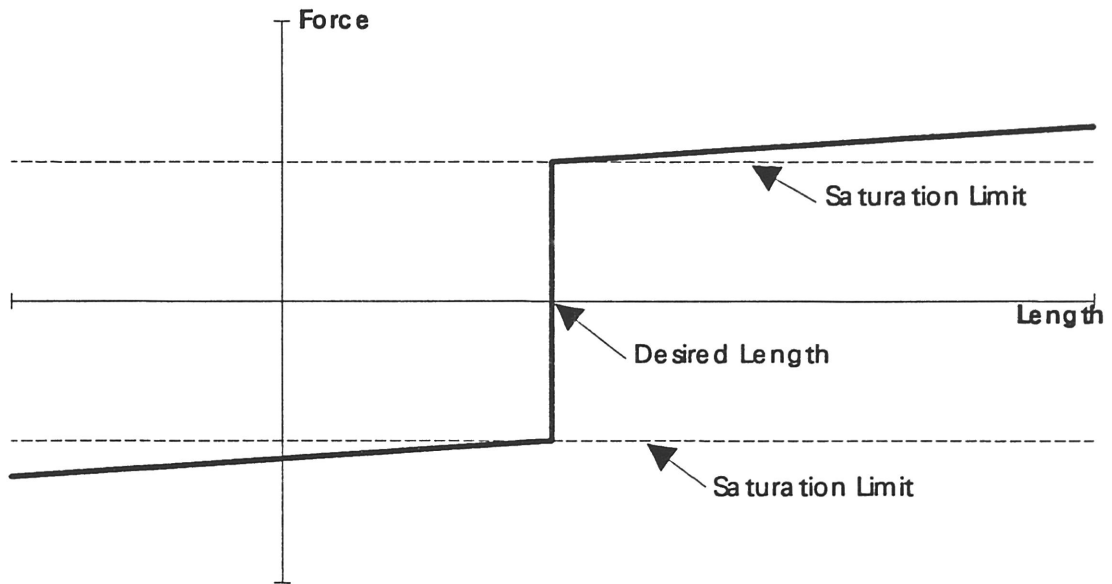


FIGURE 14: Force provided by the actuator as a function of length

From this graph, we can see that the actuator can withstand any force within a given limit to give the desired length. If the force exceeds this saturation limit, either in tension or compression, the actuator begins to change from its unsaturated length as a function of the forces acting on it. This can be put into equation form as follows:



$$\ell_{2X} = (\ell_{2X})_{\text{UNSATURATED}} + f(\text{Forces}) \quad (35)$$

where  $\ell_{2X}$  represents either  $\ell_{2A}$  and  $\ell_{2B}$   
 $f(\text{Forces})$  is a function involving the forces at either B or C and  
a compliance factor for the actuator

This equation was added to relate the desired length of the actuator to its actual length. Values were found for the remaining variables in the time step by using formulae in a scheme as described in Appendix A, Parts 2 and 3.

For the three degree-of-freedom system, values for both  $\ell_{2A}$  and  $\ell_{2B}$  were removed from the list of knowns and replaced by  $\phi$ ,  $\dot{\phi}$ ,  $x$ , and  $\dot{x}$ . Likewise, Equation (35) with two different ' $f(\text{Forces})$ ' were added, one each for  $\ell_{2A}$  and  $\ell_{2B}$ . The scheme of solving the formulae is found in Appendix A, Part 4.

Once the setup of the formulae were decided on, the simulation could begin. The initial conditions given to the system were an initial displacement and velocity of  $\theta$ . The initial length of the actuators was assumed to be the nominal length, i.e. each half of the base length.

## RESULTS

The results of these simulations proved to be unsatisfactory. Several different methods of varying the lengths of the actuators were tried. These included sinusoidally, instantaneously, along a ramp surrounding the equilibrium point, and including a hysteresis for the ramp about the equilibrium point. While these did provide for some strange and interesting dynamics, none provided any damping effects. In fact, depending on the frequency of the sinusoidal pattern, it was possible to resonate with the natural frequency of the system and add energy.

## DISCUSSION

The first thing done when all of the techniques for varying the lengths of the actuators were tried was to ensure that the program was running properly. This involved running simple

test cases where the results were known prior to running the program. These included cases such as keeping the actuator lengths constant with a given initial displacement of  $\theta$ . This gave the expected sinusoidal response for the displacement of the endmass. Then, the initial displacement of  $\theta$  was reduced to zero, and the lengths of both of the actuators were varied sinusoidally, which should allow the endmass to remain stationary. While this did cause the endmass to move, the amplitude (five orders of magnitude below that of the system) indicate that the error was probably numerical in nature rather than a problem with the program.

After ensuring that the program was running properly and becoming assured that merely changing the rotation of the endmass was not going to remove energy from the system, this method was abandoned.

## CHAPTER IV

## SPRING-DAMPER METHOD

## THEORY

The next method for controlling the oscillations of the flexible arm was to simply use springs and dampers for the connections between the end of the beams and the endmass. The springs were included to add stiffness to the system so that a force acting on the endmass would cause the whole arm to move rather than merely the endmass. Changing the natural length of these springs is also the method by which the geometry of the system is changed. The damper is the mechanism by which the energy is removed from the system. This system uses the movement of the beams and the endmass relative to each other to damp the oscillation in the system.

Assume the arm has reached the end of its motion and the base has stopped, but the endmass is displaced from its equilibrium point due to the flexibility in the beams (see Figure 15). After the base has stopped, the endmass will continue moving due to its inertia and the restoring torque in the beams as they move toward equilibrium. Once the beams pass equilibrium, they will try to reverse the direction of their motion, but the endmass will keep moving in the same direction due to its inertia (see Figure 16). This will cause a significant amount of relative motion between the beams and the endmass. The dampers use this relative motion to dissipate energy.

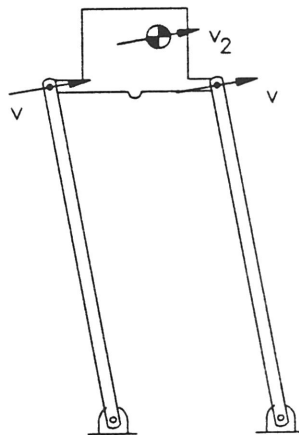


FIGURE 15: Diagram of the system immediately after base motion stops

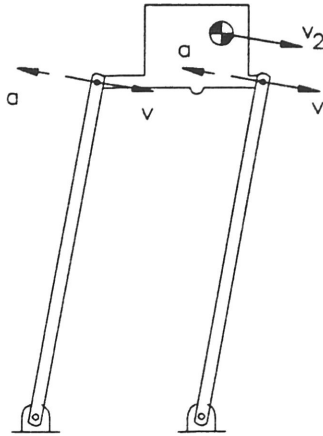


FIGURE 16: Diagram of the system with the beams past equilibrium

Also, as the beams become more in-drawn, the damping in the system should increase. This can be attributed to the fact that at least one beam is more likely to be past their equilibrium point, and thus slowing down, than for the parallel configuration (see Figure 17). Any time this happens, that damper will be dissipating energy. Thus, the more often this happens, the more damping will occur. However, increasing the offset angle also increases the rotational motion, which is not used in dissipating energy, and will increase the settling time.

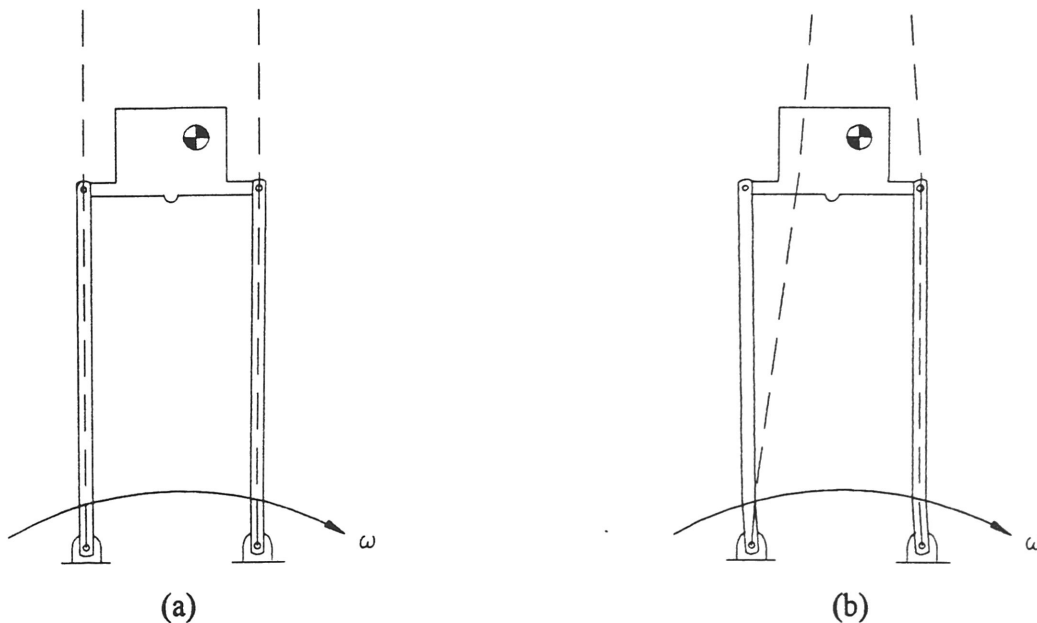


FIGURE 17: Point of passing equilibrium for a) Parallel and b) In-drawn configuration

It is also understood that the damping by this system is going to be dependent on the mass, mass moment of inertia, and location of the center of gravity for the endmass. The exact relationship is rather vague, but general hypotheses have been developed. As mass of the endmass increases, settling time should increase because of the increased momentum that is gained during movement. As the mass moment of inertia of the endmass increases, settling time should decrease. This is due to the fact that added moment of inertia will let the beams move much more relative to the endmass, allowing the dampers to dissipate more energy without having extra mass to build the momentum. The same logic applies to locating the center of gravity further from the beams.

## SIMULATION

Again, finding the number of degrees of freedom was the first objective for the system. Because the lengths of  $\ell_{2A}$  and  $\ell_{2B}$  are not known, there are three degrees of freedom. The three state vectors to correspond to these three degrees of freedom are  $\theta$  for the first beam,  $\phi$  for the second beam, and  $x$  for the endmass. The equations can be arranged into a scheme where initial conditions are the displacement and velocity vectors are known for  $\theta$ ,  $\phi$ , and  $x$ , and results are ultimately found for the second derivatives of these variables. These results are then integrated twice to proceed to the next time step. This scheme can be found in Appendix B.

Once the general scheme had been determined, the simulation was performed. The initial conditions were again an initial displacement and velocity in  $\theta$ , with the initial lengths of  $\ell_{2A}$  and  $\ell_{2B}$  being set to the natural length of the springs in those connections. These lengths varied depending upon how much the beams were to be in-drawn.

The results of these simulations looked promising. As expected, the oscillations were removed within a reasonable amount of time (10-20 seconds). At this point, analysis showed that any two situations could not be compared due to the differences in stored energy at time  $t=0$ . This value differed according to how much the beams were in-drawn. This can be seen in Figure 18. For the same initial conditions for  $\theta$ , as the beams become more and more in-drawn, the

amount of stored energy increases. Naturally, a system with more initial energy will take a longer amount of time to settle. Therefore, it was decided to put energy into the system by storing it in the springs connecting the beams and the endmass. This was done by displacing the endmass close to one of the beams while starting the beams in their equilibrium position. In this way, the only stored energy was that found in the springs between the endmass and the ends of the beams.

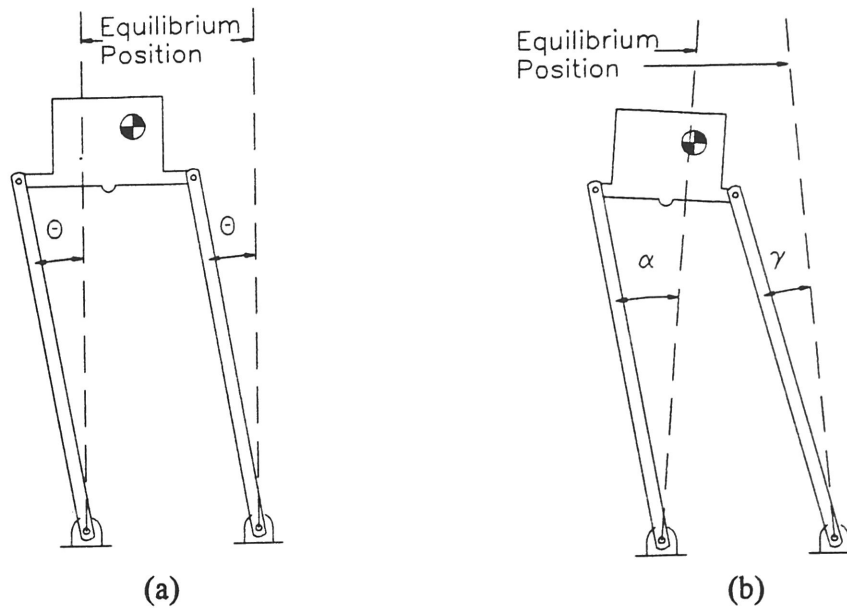


FIGURE 18: Displacement from equilibrium for a) Parallel and b) In-drawn beams for a given initial  $\theta$  displacement

However, if this is to work, the natural length of the connecting springs must remain constant from simulation to simulation. This means that configuration cannot be made in-drawn by making the equilibrium position for the ends of the beams closer to the endmass. Instead, the base length must be increased.

This method was run varying each of several components. For the purpose of determining the effect of each component, simulations were run for combinations of three endmasses, and each of these was run with three different center of gravity displacements. The center of gravity displacements were calculated by changing the overall mass moment of inertia while assuming that

the mass moment of inertia of the endmass itself remained constant. Assuming that the displacements were all in the  $d_1$  direction (away from the base), the formula for finding  $d_1$  is

$$d_1 = \left( \frac{I_2 - J}{m_2} \right)^{1/2} \quad (36)$$

where  $I_2$  is the given mass moment of inertia  
 $J$  is the mass moment of inertia of the endmass

These nine combinations were run for each of six different configurations. The configurations differed in the offset angle, defined as the angle from the y-direction at which the beam is at equilibrium. Also at equilibrium, the springs was at their natural length. By this definition, parallel beams were at a configuration of  $0^\circ$ . The values used for these variables is listed below.

Mass : 1 kg, 7 kg, 15 kg

Mass moment of inertia: 0.25 kg·m<sup>2</sup> ( $d_1 = 0$ ), 0.50 kg·m<sup>2</sup>, 0.75 kg·m<sup>2</sup>

Configurations:  $0^\circ$ ,  $2^\circ$ ,  $4^\circ$ ,  $6^\circ$ ,  $8^\circ$ ,  $10^\circ$

This gave a total of 54 simulations performed. For each of these simulations, information concerning the displacement and velocity of  $\theta$ ,  $\phi$ , and  $x$  were recorded. Also recorded was data on the forces felt in each of the pins, the logarithmic decrement of  $x$ , the rotational displacement and velocity of the endmass, and the lengths and rate of change of the lengths of  $\ell_{2A}$  and  $\ell_{2B}$ .

## RESULTS

Although a great deal of data was recorded for each simulation that was run, not all of it was immediately applicable. Of immediate interest was the information concerning the motion of the endmass. This was characterized by a settling time and a peak value. This information is presented below in Tables 1-3. These tables show the maximum overshoot of the endmass past its equilibrium position ( $x_0$ ) and the time required to settle to within 0.5% of the final value ( $t_s$ ).

Each of the tables represents a different  $I_2$ , which correspond to different  $d_1$ 's. Within each table, columns represent constant mass, and rows represent constant offset angles.

	m = 1 kg	m = 7 kg	m = 15 kg
Offset = 0°	$x_o = 1.05$ cm $t_s = 0.75$ s	$x_o = 2.5$ cm $t_s = 4.01$ s	$x_o = 2.93$ cm $t_s = 9.09$ s
Offset = 2°	$x_o = 1.11$ cm $t_s = 0.87$ s	$x_o = 2.5$ cm $t_s = 4.38$ s	$x_o = 2.935$ cm $t_s = 9.09$ s
Offset = 4°	$x_o = 1.17$ cm $t_s = 1.31$ s	$x_o = 2.5$ cm $t_s = 4.39$ s	$x_o = 2.93$ cm $t_s = 9.11$ s
Offset = 6°	$x_o = 1.06$ cm $t_s = 2.51$ s	$x_o = 2.48$ cm $t_s = 4.41$ s	$x_o = 2.90$ cm $t_s = 9.13$ s
Offset = 8°	$x_o = 0.87$ cm $t_s = 5.25$ s	$x_o = 2.49$ cm $t_s = 4.82$ s	$x_o = 2.88$ cm $t_s = 9.16$ s
Offset = 10°	$x_o = 0.674$ cm $t_s = 10.7$ s	$x_o = 2.5$ cm $t_s = 5.25$ s	$x_o = 2.84$ cm $t_s = 9.74$ s

TABLE 1: Overshoot and settling time for  $I_2 = 0.25$  kg·m<sup>2</sup>

	m = 1 kg	m = 7 kg	m = 15 kg
Offset = 0°	$x_o = 1.05$ cm $t_s = 0.75$ s	$x_o = 2.5$ cm $t_s = 4.01$ s	$x_o = 2.94$ cm $t_s = 9.09$ s
Offset = 2°	$x_o = 0.841$ cm $t_s = 0.65$ s	$x_o = 2.4$ cm $t_s = 3.92$ s	$x_o = 2.88$ cm $t_s = 8.42$ s
Offset = 4°	$x_o = 3.63$ cm $t_s = 3.43$ s	$x_o = 2.3$ cm $t_s = 3.49$ s	$x_o = 2.82$ cm $t_s = 7.77$ s
Offset = 6°	UNSTABLE	$x_o = 2.29$ cm $t_s = 3.42$ s	$x_o = 2.735$ cm $t_s = 7.66$ s
Offset = 8°	UNSTABLE	$x_o = 1.975$ cm $t_s = 3.01$ s	$x_o = 2.75$ cm $t_s = 7.05$ s
Offset = 10°	UNSTABLE	$x_o = 1.56$ cm $t_s = 2.05$ s	$x_o = 2.63$ cm $t_s = 6.95$ s

TABLE 2: Overshoot and settling time for  $I_2 = 0.5$  kg·m<sup>2</sup>



	m = 1 kg	m = 7 kg	m = 15 kg
Offset = 0°	$x_o = 1.06$ cm $t_s = 0.75$ s	$x_o = 2.5$ cm $t_s = 4.01$ s	$x_o = 2.94$ cm $t_s = 9.09$ s
Offset = 2°	$x_o = 0.706$ cm $t_s = 0.81$ s	$x_o = 2.36$ cm $t_s = 3.53$ s	$x_o = 2.86$ cm $t_s = 7.84$ s
Offset = 4°	UNSTABLE	$x_o = 2.26$ cm $t_s = 3.43$ s	$x_o = 2.78$ cm $t_s = 7.67$ s
Offset = 6°	UNSTABLE	$x_o = 2.03$ cm $t_s = 2.97$ s	$x_o = 2.71$ cm $t_s = 7.01$ s
Offset = 8°	UNSTABLE	$x_o = 1.6$ cm $t_s = 5.46$ s	$x_o = 2.59$ cm $t_s = 6.36$ s
Offset = 10°	UNSTABLE	UNSTABLE	$x_o = 2.18$ cm $t_s = 5.82$ s

TABLE 3: Overshoot and settling time for  $I_2 = 0.75 \text{ kg}\cdot\text{m}^2$

From the information in these tables, certain trends were found as functions of changes in the mass of the endmass, the displacement of the center of gravity of the endmass, and the offset angle of the beams. Some of these trends are represented below. Shown as well are the two typical displacements of the endmass from its equilibrium point as a function of time.

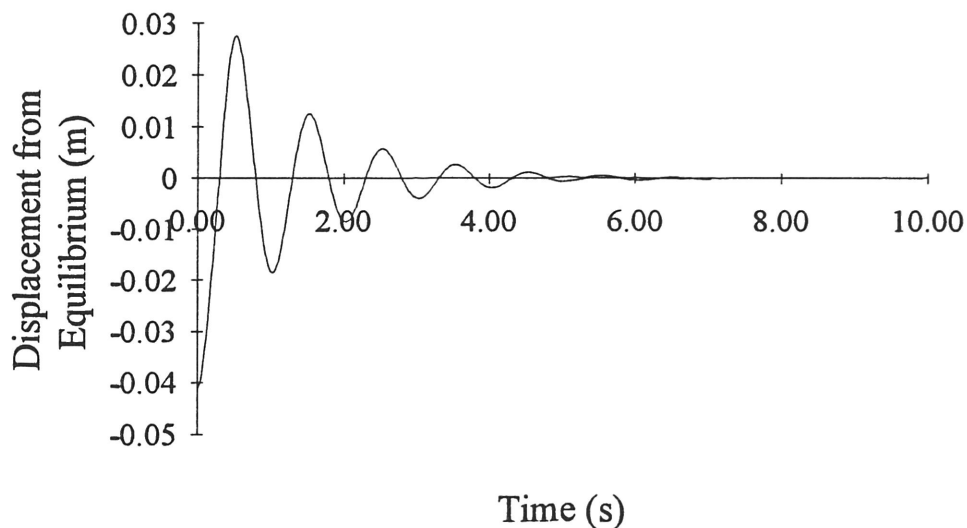


FIGURE 19: Typical plot of the displacement of the endmass from equilibrium as a function of time for a stable system

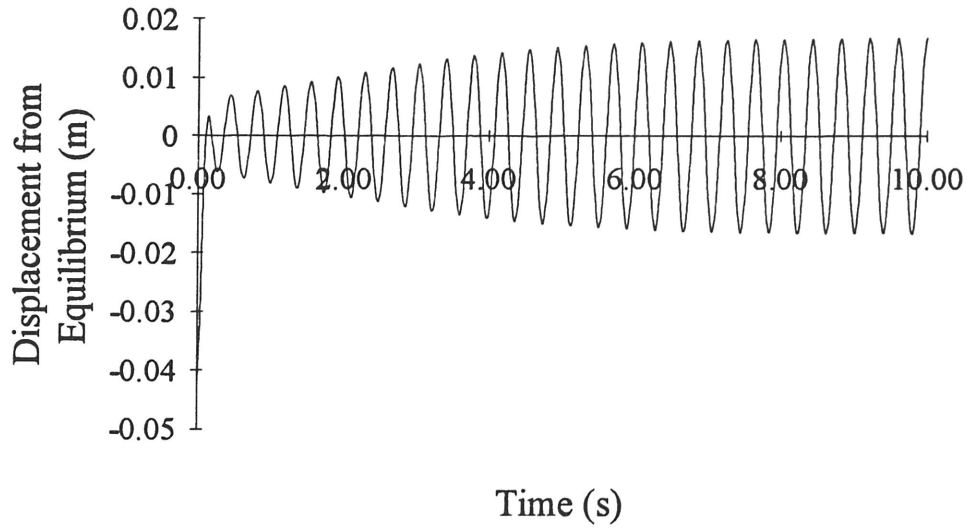


FIGURE 20: Typical plot of the displacement of the endmass from equilibrium as a function of time for an unstable system

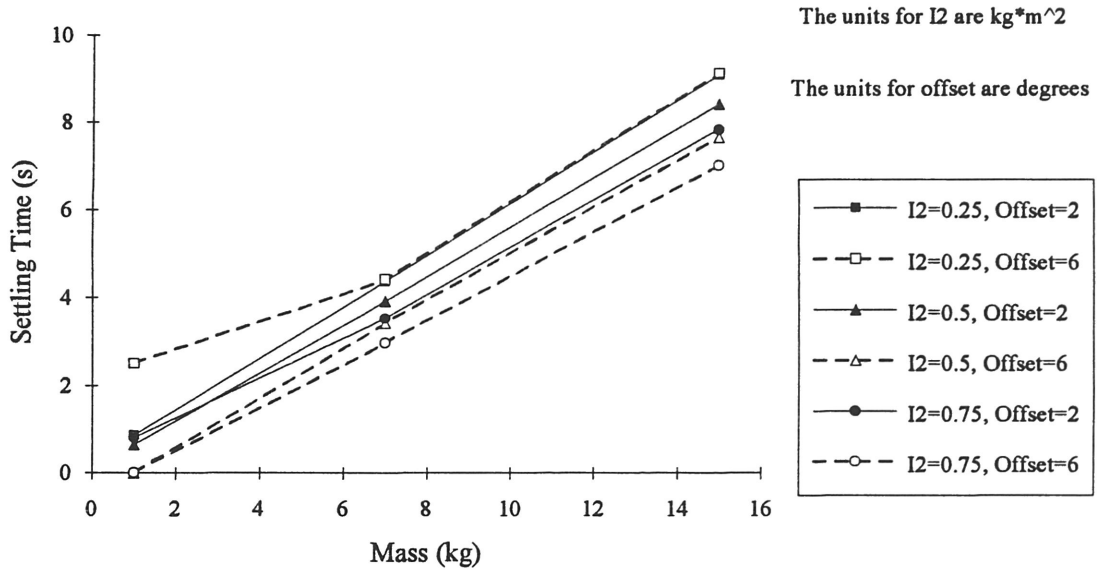


FIGURE 21: Endmass settling time as a function of mass

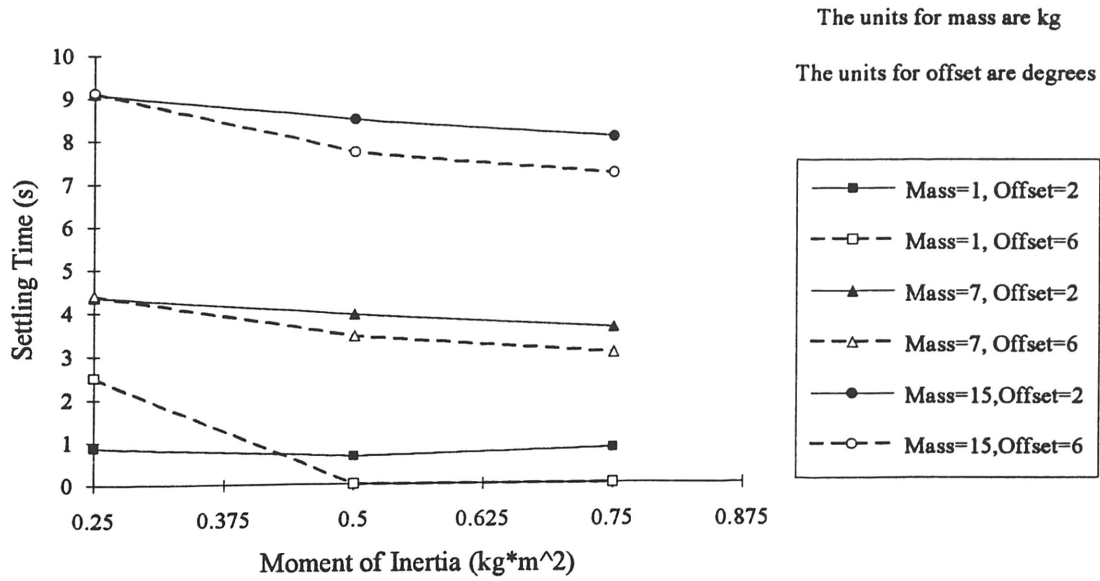


FIGURE 22: Endmass settling time as a function of distance to the center of gravity ( $d_1$ )

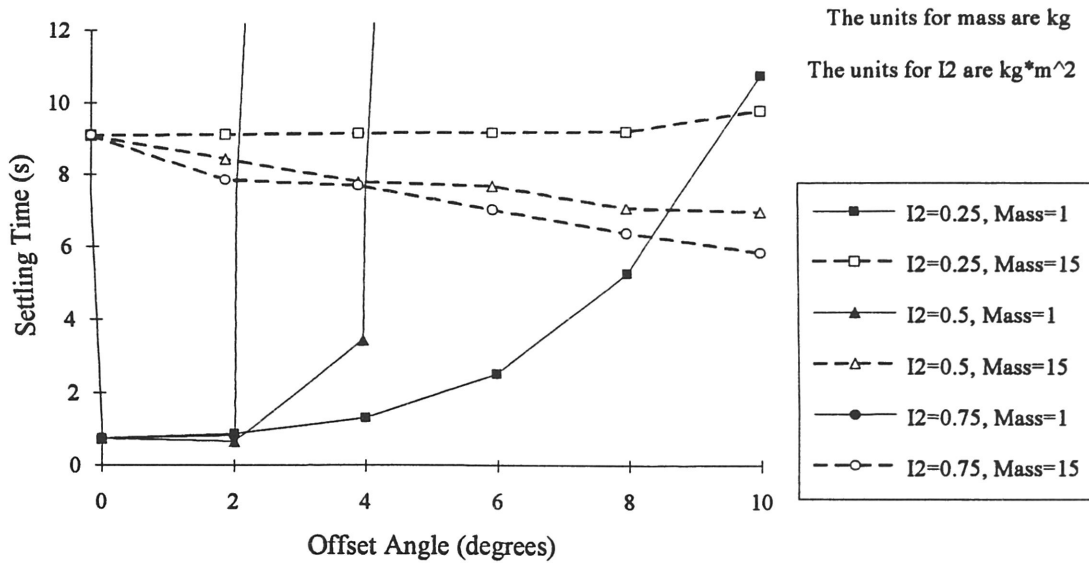


FIGURE 23: Endmass settling time as a function of configuration

Also of interest was some method of quantifying the damping achieved by the system. This was done by taking the logarithmic decrement of  $x$ , the displacement of the endmass from its equilibrium position. This value was found using the formula

$$\delta = \frac{1}{2} \ln \left( \frac{x_0}{x_2} \right) \quad (37)$$

where  $\delta$  is the logarithmic decrement

$x_0$  is the value of the first peak of the displacement of the endmass

$x_2$  is the value of the third peak of the displacement of the endmass

## DISCUSSION

While the tables provide a great deal of information, of more interest are the implications of several of the trends found within those tables, some of which are shown in Figures 19-23. For instance, it is interesting to note that for the parallel beams (Offset = 0°), there was no decrease in settling time for an increase the mass moment of inertia. However, as the offset angle increases, the settling time began to decrease for a non-zero value of  $d_1$ , as given by the mass moment of inertia. One possible reason for this is that as the offset angle increases, rotational motion tends to increase; yet, for a center of gravity placed a finite distance from the ends of the two beams, it becomes more difficult to rotate the endmass. Thus, although the beams are oscillating, the endmass cannot rotate at the same rate. This corresponds to increased movement of the beams in relation to the endmass, increasing the amount of energy dissipated by the dampers.

This theory also explains the decrease in settling time which results from increasing the mass moment of inertia by increasing the distance to the center of gravity. For a given amount of rotational motion, as the distance to the center of gravity increases, the resistance to the rotation will increase. This increases the relative motion between the endmass and the beams, allowing more energy to be dissipated by the dampers.

An expected trend is the increase in settling time that results from having a greater mass. This is because of the momentum gained as the endmass moves from the initial displacement; more energy is required to cause it to change direction than would be necessary for a smaller mass. This adds credibility to the simulation.

One disturbing thing is results obtained for having no distance to the center of gravity ( $I_2 = 0.25 \text{ kg}\cdot\text{m}^2$ ). These results exhibit the opposite trend for settling time as the offset angle increases. One possible explanation is that the forces acting at pins B and C would for this case act directly from the spring and damper through the center of gravity. This would greatly reduce, if not completely eliminate, the amount of rotation produced by the oscillation of the arm. Then, as the offset angle was increased and the motion went from translational to rotational, the energy dissipated by the dampers would decrease, requiring a longer amount of time to settling to within 0.5% of the final value. Fortunately, this is a very unlikely situation because most endmasses will be composed of either additional links, manipulators, or workpieces, which will give a center of gravity some finite distance away from between the ends of the beams.

Another disturbing aspect of the data presented is the "unstable" systems found for high  $d_1$ , low mass, high offset angle situations. Because an unstable system is an impossibility due to the lack of inputted energy into the system, this is most likely due to a numerical instability in the program. In reality, this type of system would probably have very little or no damping rather than the instability.

## CHAPTER V

### CONCLUSION

#### SUMMARY

In the end, damping was achieved in the system. Although the initial method of removing the oscillations (the actuator method) did not achieve the desired results, a method was found (the spring-damper method) which did. In addition, the system had the ability to achieved a fairly quick settling time considering the fact that no other damping was modeled into the system. Also, the behavior of the displacement of endmass followed the expected trend for an increase in mass and distance to the center of gravity. Furthermore, the addition of beam offset angles into the configuration was shown to have added benefits in terms of settling time and overshoot.

Another positive aspect of the spring-damper system is its passiveness: no inputs are required whatsoever. This includes feedback or even power. This means that the chances of failure are reduced. Also, because the springs, at least for these simulations, were modeled as having the same stiffness as the flexible beams, any deflection will be a result of bending of the beams as well as compression/extension of the springs.

So, overall, the flexible arm with dual-beam links has possibilities for implementation. Although it will weigh more than one with single-beam links, the arm will still weigh much less than an equivalent stiff-link arm. Furthermore, the dual-beam link has the benefit of the simplicity that results from a completely passive system.

#### RECOMMENDATIONS FOR FUTURE STUDY

Analysis of the remaining data collected for the simulation needs to be done, including the rotation of the endmass and the forces acting at the pins. Also, experimental work needs to be done to determine if a real system performs reasonably close to the theoretical system. This could be done using the flexible arm located at Texas A&M University, although, because it is two-link, modifications could probably be made to simplify the system.

If the real system performs close to the prediction, then an effort should be made to develop a more accurate model of the system. This would include using beam analysis or possibly finite elements rather than the pseudolink method in modeling the beams. Also, some compliance can be given to the base to allow for compliance of the motor.

If an accurate model for the system can be developed, other factors could be included which may aid in removing the oscillations. One possibility includes having the forces at B and C at equilibrium be a finite value rather than zero. These further investigations should also try to differentiate between changing the mass moment of inertia of the endmass and the position of the center of gravity.

## REFERENCES

1. Nathan, P.J., and Sahjendra N. Singh. "Nonlinear Ultimate Boundedness Control and Stabilization of a Flexible Robotic Arm." *Journal of Robotic Systems*. Vol. 9, no. 3, pp. 301-326, 1992.
2. Jankowski, Krzysztof P. and Hendrik Van Brussel. "An Approach to Discrete Inverse Dynamics Control of Flexible-Joint Robots." *IEEE Transactions on Robotics and Automation*. Vol. 8, no. 5, pp. 651-658, October 1992.
3. Madhavan, Sethu K. and Sahjendra N. Singh. "Variable Structure Trajectory Control of an Elastic Robotic Arm." *Journal of Robotic Systems*. Vol. 10, no. 1, pp. 23-44, 1993.
4. Mahmood, Niaz and Bruce L. Walcott. "Computer-Aided VSS Control Validation for a Rotating Flexible Link Manipulator Using ANSYS." *Simulation*. Vol. 60, no. 1, pp. 54-62, January 1993.
5. Shelburne, Kevin Barry. "Variable Structure Control of a Flexible Manipulator." *Master's Thesis*, Department of Mechanical Engineering, Texas A&M University, December 1988.
6. Wang, David and M. Vidyasagar, "Passive Control of Stiff Flexible Link." *The International Journal of Robotics Research*. Vol. 11, no. 6, pp. 572-578, December 1992.
7. Fancello, Angelo. "The Design and Modeling of a Compliant Manipulator." *Master's Thesis*, Department of Mechanical Engineering, Texas A&M University, August 1988.



## APPENDIX A

## EQUATIONS FOR THE ACTUATOR METHOD

## PART 1

The first possible situation for the actuator method is that both of the actuators are unsaturated, giving a one degree-of-freedom system. For this case, only the equations given in the modeling portion of the text are used for the equations.

The initial conditions for this situation are given values for  $\theta, \dot{\theta}, l_{2A}, l_{2B}, \dot{l}_{2A}, \dot{l}_{2B}, \ddot{l}_{2A}$ , and  $\ddot{l}_{2B}$ . To get started, we must for a moment assume that  $\beta$  is a small angle. With this assumption, we can simplify Eqn. (30) from the text to get

$$\phi = \sin^{-1} \left[ \frac{L - l_1 \sin \theta - (l_{2A} + l_{2B})}{l_3} \right] \quad (\text{A1-1})$$

The value obtained from this calculation will go directly into Eqn. (26) from the text to give

$$\beta = \sin^{-1} \left[ \frac{l_3 \cos \phi - l_1 \cos \theta}{l_{2A} + l_{2B}} \right] \quad (\text{A1-2})$$

From there, Eqns. (27) and (31) are solved simultaneously. After combination, the two equations become

$$\phi = \frac{1}{l_3 \cos(\beta - \phi)} \left[ -l_1 \dot{\theta} \cos(\beta + \theta) - (\dot{l}_{2A} + \dot{l}_{2B}) \right] \quad (\text{A1-3})$$

$$\dot{\beta} = \frac{1}{(l_{2A} + l_{2B}) \cos \beta} \left[ l_1 \dot{\theta} \sin \theta - l_3 \dot{\phi} \sin \phi - (\dot{l}_{2A} + \dot{l}_{2B}) \sin \beta \right] \quad (\text{A1-4})$$

Using these values plus the initial conditions, the rest of the equations must be solved simultaneously. The variables to be solved for include  $\ddot{\theta}, \ddot{\phi}, \ddot{\beta}, B_x, B_y, C_x$ , and  $C_y$

The equations will be set up in the following manner:

$$[\tilde{A}] \cdot [\tilde{x}] = [\tilde{C}]$$

where, for this situation,

$$[\tilde{A}] = \begin{bmatrix} \frac{1}{3} m_1 \ell_1^2 & 0 & 0 & -\ell_1 \cos \theta & \ell_1 \sin \theta & 0 & 0 \\ 0 & \frac{1}{3} m_3 \ell_3^2 & 0 & 0 & 0 & -\ell_3 \cos \phi & \ell_3 \sin \phi \\ -\ell_1 \cos \theta & 0 & \ell_{2A} \sin \beta + d_1 \cos \beta + d_2 \sin \beta & -\frac{1}{m_2} & 0 & \frac{1}{m_2} & 0 \\ \ell_1 \sin \theta & 0 & -(\ell_{2A} \cos \beta - d_1 \sin \beta + d_2 \cos \beta) & 0 & -\frac{1}{m_2} & 0 & -\frac{1}{m_2} \\ 0 & 0 & -I_2 & -(\ell_{2A} \sin \beta + d_1 \cos \beta + d_2 \sin \beta) & \ell_{2A} \cos \beta - d_1 \sin \beta + d_2 \cos \beta & -\ell_{2B} \sin \beta - d_1 \cos \beta + d_2 \sin \beta & -\ell_{2B} \cos \beta - d_1 \sin \beta + d_2 \cos \beta \\ -\ell_1 \sin \theta & \ell_3 \sin \phi & -(\ell_{2A} + \ell_{2B}) \cos \beta & 0 & 0 & 0 & 0 \\ \ell_1 \cos \theta & \ell_3 \cos \phi & -(\ell_{2A} + \ell_{2B}) \sin \beta & 0 & 0 & 0 & 0 \end{bmatrix}$$

$$[\tilde{x}] = \begin{bmatrix} \ddot{\theta} \\ \ddot{\phi} \\ \ddot{\beta} \\ B_x \\ B_y \\ C_x \\ C_y \end{bmatrix}$$

$$[\tilde{C}] = \begin{bmatrix} -k_1 \theta \\ -k_3 \phi \\ -\ell_1 \dot{\theta}^2 \sin \theta + \ddot{\ell}_{2A} \cos \beta - 2\dot{\ell}_{2A} \dot{\beta} \sin \beta - \dot{\beta}^2 (\ell_{2A} \cos \beta - d_1 \sin \beta + d_2 \cos \beta) \\ -\ell_1 \dot{\theta}^2 \cos \theta + \ddot{\ell}_{2A} \sin \beta + 2\dot{\ell}_{2A} \dot{\beta} \cos \beta - \dot{\beta}^2 (\ell_{2A} \sin \beta + d_1 \cos \beta + d_2 \sin \beta) \\ 0 \\ \ell_1 \dot{\theta}^2 \cos \theta - (\ddot{\ell}_{2A} + \ddot{\ell}_{2B}) \sin \beta - 2(\dot{\ell}_{2A} + \dot{\ell}_{2B}) \dot{\beta} \cos \beta + (\ell_{2A} + \ell_{2B}) \dot{\beta}^2 \sin \beta - \ell_3 \dot{\phi}^2 \cos \phi \\ \ell_1 \dot{\theta}^2 \sin \theta - (\ddot{\ell}_{2A} + \ddot{\ell}_{2B}) \cos \beta + 2(\dot{\ell}_{2A} + \dot{\ell}_{2B}) \dot{\beta} \sin \beta + (\ell_{2A} + \ell_{2B}) \dot{\beta}^2 \cos \beta + \ell_3 \dot{\phi}^2 \sin \phi \end{bmatrix}$$

## PART 2

Another possible schematic for the actuator method is if actuator  $\ell_{2A}$  is saturated. When an actuator is saturated, the actual length differs from the desired length as a function of the forces acting on it. When this happens,  $\ell_{2A}$ ,  $\dot{\ell}_{2A}$ , and  $\ddot{\ell}_{2A}$  are unknown. This gives the system two degrees of freedom. As such, integration of two state variables must be performed. In this case,  $\phi$  was chosen as the other state variable. This makes the initial conditions for this situation  $\theta, \dot{\theta}, \phi, \dot{\phi}, \ell_{2B}, \dot{\ell}_{2B}$ , and  $\ddot{\ell}_{2B}$ .

To begin to solve this set of equations, Equations (25) and (29) are combined to give

$$\beta = \tan^{-1} \left[ \frac{L - \ell_1 \sin \theta - \ell_3 \sin \phi}{\ell_3 \cos \phi - \ell_1 \cos \theta} \right] \quad (\text{A2-1})$$

Then using Equation (25) again gives

$$\ell_{2A} = \frac{\ell_3 \cos \phi - \ell_1 \cos \theta - \ell_{2B} \sin \beta}{\sin \beta} \quad (\text{A2-2})$$

Then Equation (A1-3) can be rearranged algebraically and Equation (A1-4) used directly to give

$$\dot{\ell}_{2A} = -\ell_1 \dot{\theta} \cos(\beta + \phi) - \ell_3 \dot{\phi} \cos(\beta - \phi) - \dot{\ell}_{2B} \quad (\text{A2-3})$$

$$\dot{\beta} = \frac{1}{(\ell_{2A} + \ell_{2B}) \cos \beta} \left[ \ell_1 \dot{\theta} \sin \theta - \ell_3 \dot{\phi} \sin \phi - (\dot{\ell}_{2A} + \dot{\ell}_{2B}) \sin \beta \right] \quad (\text{A2-4})$$

Again, the remaining equations must be solved simultaneously. The matrices used in this situation are very similar to those used in the previous part. The difference is the addition of  $\dot{\ell}_{2A}$  to the unknowns. This additional unknown is balanced by the equation which approximates the saturated length of the actuator based on the forces acting along it. This gives the equation

$$\ell_{2A} - (\ell_{2A})_{\text{UNSATURATED}} = \frac{1}{\text{Stiff}} (B_x \cos \beta + B_y \sin \beta) \quad (\text{A2-5})$$

where Stiff is the stiffness of the actuator when saturated

which combines with the other equations to give the following system of equations to solve simultaneously:

$$[\tilde{A}] = \begin{bmatrix} \frac{1}{3}m_1\ell_1^2 & 0 & 0 & -\ell_1 \cos\theta & \ell_1 \sin\theta & 0 & 0 & 0 \\ 0 & \frac{1}{3}m_3\ell_3^2 & 0 & 0 & 0 & -\ell_3 \cos\phi & \ell_3 \sin\phi & 0 \\ -\ell_1 \cos\theta & 0 & \ell_{2A} \sin\beta + d_1 \cos\beta + d_2 \sin\beta & -\frac{1}{m_2} & 0 & \frac{1}{m_2} & 0 & -\cos\beta \\ \ell_1 \sin\theta & 0 & -(\ell_{2A} \cos\beta - d_1 \sin\beta + d_2 \cos\beta) & 0 & -\frac{1}{m_2} & 0 & -\frac{1}{m_2} & -\sin\beta \\ 0 & 0 & -I_2 & -(\ell_{2A} \sin\beta + d_1 \cos\beta + d_2 \sin\beta) & \ell_{2A} \cos\beta - d_1 \sin\beta + d_2 \cos\beta & -\ell_{2B} \sin\beta - d_1 \cos\beta + d_2 \sin\beta & -\ell_{2B} \cos\beta - d_1 \sin\beta + d_2 \cos\beta & 0 \\ -\ell_1 \sin\theta & \ell_3 \sin\phi & -(\ell_{2A} + \ell_{2B}) \cos\beta & 0 & 0 & 0 & 0 & \sin\beta \\ \ell_1 \cos\theta & \ell_3 \cos\phi & -(\ell_{2A} + \ell_{2B}) \sin\beta & 0 & 0 & 0 & 0 & \cos\beta \\ 0 & 0 & 0 & \frac{1}{\text{Stiff}} \cos\beta & \frac{1}{\text{Stiff}} \sin\beta & 0 & 0 & 0 \end{bmatrix}$$

$$[\tilde{x}] = \begin{bmatrix} \ddot{\theta} \\ \ddot{\phi} \\ \ddot{\beta} \\ B_x \\ B_y \\ C_x \\ C_y \\ \ddot{\ell}_{2A} \end{bmatrix}$$

$$[\tilde{C}] = \begin{bmatrix} -k_1\theta \\ -k_3\phi \\ -\ell_1 \dot{\theta}^2 \sin\theta - 2\dot{\ell}_{2A} \dot{\beta} \sin\beta - \dot{\beta}^2 (\ell_{2A} \cos\beta - d_1 \sin\beta + d_2 \cos\beta) \\ -\ell_1 \dot{\theta}^2 \cos\theta + 2\dot{\ell}_{2A} \dot{\beta} \cos\beta - \dot{\beta}^2 (\ell_{2A} \sin\beta + d_1 \cos\beta + d_2 \sin\beta) \\ 0 \\ \ell_1 \dot{\theta}^2 \cos\theta - \ddot{\ell}_{2B} \sin\beta - 2(\dot{\ell}_{2A} + \dot{\ell}_{2B}) \dot{\beta} \cos\beta + (\ell_{2A} + \ell_{2B}) \dot{\beta}^2 \sin\beta - \ell_3 \dot{\phi}^2 \cos\phi \\ \ell_1 \dot{\theta}^2 \sin\theta - \ddot{\ell}_{2B} \cos\beta + 2(\dot{\ell}_{2A} + \dot{\ell}_{2B}) \dot{\beta} \sin\beta + (\ell_{2A} + \ell_{2B}) \dot{\beta}^2 \cos\beta + \ell_3 \dot{\phi}^2 \sin\phi \\ \ell_{2A} - (\ell_{2A})_{\text{UNSATURATED}} \end{bmatrix}$$

## PART 3

The third possible situation for the system when using the actuator method is very similar to the situation in Part 2. The only difference is that the  $\ell_{2B}$  actuator is being saturated rather than the  $\ell_{2A}$  actuator. This changes the initial conditions slightly to be  $\theta, \dot{\theta}, \phi, \dot{\phi}, \ell_{2A}, \dot{\ell}_{2A}$ , and  $\ddot{\ell}_{2A}$ , but the system still has two degrees of freedom. Also, the variable  $\phi$  is chosen as the other state variable.

The equations used to solve for the other variables in the system also are very close to those in Part 2. The first is actually a direct copy of Equation (A2-1)

$$\beta = \tan^{-1} \left[ \frac{L - \ell_1 \sin \theta - \ell_3 \sin \phi}{\ell_3 \cos \phi - \ell_1 \cos \theta} \right] \quad (\text{A3-1})$$

The next two equations are in fact the same as Equations (A2-2) and (A2-3); the only difference is the variable for which it is being used to solve.

$$\ell_{2B} = \frac{\ell_3 \cos \phi - \ell_1 \cos \theta - \ell_{2A} \sin \beta}{\sin \beta} \quad (\text{A3-2})$$

$$\dot{\ell}_{2B} = -\ell_1 \dot{\theta} \cos(\beta + \phi) - \ell_3 \dot{\phi} \cos(\beta - \phi) - \dot{\ell}_{2A} \quad (\text{A3-3})$$

The final variable being solved for uses another equation directly from Part 2 in the form of Equation (A2-4).

$$\dot{\beta} = \frac{1}{(\ell_{2A} + \ell_{2B}) \cos \beta} \left[ \ell_1 \dot{\theta} \sin \theta - \ell_3 \dot{\phi} \sin \phi - (\dot{\ell}_{2A} + \dot{\ell}_{2B}) \sin \beta \right] \quad (\text{A3-4})$$

Again, the remaining equations must be solved simultaneously. The matrices used in this situation are almost identical to those used in the previous part. However, for this case,  $\dot{\ell}_{2B}$  is being solved for rather than  $\dot{\ell}_{2A}$ . This changes the equation defining the length of the saturated actuator to

$$\ell_{2A} - (\ell_{2A})_{\text{UNSATURATED}} = \frac{1}{\text{Stiff}} (B_x \cos \beta + B_y \sin \beta) \quad (\text{A3-5})$$

which combines with the other equations to give the following system of equations to solve simultaneously:

$$[\tilde{A}] = \begin{bmatrix} \frac{1}{3}m_1\ell_1^2 & 0 & 0 & -\ell_1 \cos\theta & \ell_1 \sin\theta & 0 & 0 & 0 \\ 0 & \frac{1}{3}m_3\ell_3^2 & 0 & 0 & 0 & -\ell_3 \cos\phi & \ell_3 \sin\phi & 0 \\ & & \ell_{2A} \sin\beta & & & & & \\ -\ell_1 \cos\theta & 0 & +d_1 \cos\beta & -\frac{1}{m_2} & 0 & \frac{1}{m_2} & 0 & 0 \\ & & +d_2 \sin\beta & & & & & \\ \ell_1 \sin\theta & 0 & -(\ell_{2A} \cos\beta & 0 & -\frac{1}{m_2} & 0 & -\frac{1}{m_2} & 0 \\ & & -d_1 \sin\beta + & & & & & \\ & & d_2 \cos\beta) & & & & & \\ & & & -(\ell_{2A} \sin\beta & \ell_{2A} \cos\beta & \ell_{2B} \sin\beta & -\ell_{2B} \cos\beta & \\ 0 & 0 & -I_2 & +d_1 \cos\beta & -d_1 \sin\beta & -d_1 \cos\beta & -d_1 \sin\beta & 0 \\ & & & +d_2 \sin\beta) & +d_2 \cos\beta & -d_2 \sin\beta & +d_2 \cos\beta & \\ -\ell_1 \sin\theta & \ell_3 \sin\phi & (\ell_{2A} + \ell_{2B}) \cos\beta & 0 & 0 & 0 & 0 & \sin\beta \\ \ell_1 \cos\theta & \ell_3 \cos\phi & -(\ell_{2A} + \ell_{2B}) \sin\beta & 0 & 0 & 0 & 0 & \cos\beta \\ 0 & 0 & 0 & 0 & 0 & \frac{1}{\text{Stiff}} \cos\beta & -\frac{1}{\text{Stiff}} \sin\beta & 0 \end{bmatrix}$$

$$[\tilde{x}] = \begin{bmatrix} \ddot{\theta} \\ \ddot{\phi} \\ \ddot{\beta} \\ B_x \\ B_y \\ C_x \\ C_y \\ \ddot{\ell}_{2B} \end{bmatrix}$$

$$[\tilde{C}] = \begin{bmatrix} -k_1\theta \\ -k_3\phi \\ -\ell_1 \dot{\theta}^2 \sin\theta + \ddot{\ell}_{2A} \cos\beta - 2\dot{\ell}_{2A} \dot{\beta} \sin\beta - \dot{\beta}^2 (\ell_{2A} \cos\beta - d_1 \sin\beta + d_2 \cos\beta) \\ -\ell_1 \dot{\theta}^2 \cos\theta + \ddot{\ell}_{2A} \sin\beta + 2\dot{\ell}_{2A} \dot{\beta} \cos\beta - \dot{\beta}^2 (\ell_{2A} \sin\beta + d_1 \cos\beta + d_2 \sin\beta) \\ 0 \\ \ell_1 \dot{\theta}^2 \cos\theta - \ddot{\ell}_{2A} \sin\beta - 2(\dot{\ell}_{2A} + \dot{\ell}_{2B}) \dot{\beta} \cos\beta + (\ell_{2A} + \ell_{2B}) \dot{\beta}^2 \sin\beta - \ell_3 \dot{\phi}^2 \cos\phi \\ \ell_1 \dot{\theta}^2 \sin\theta - \ddot{\ell}_{2A} \cos\beta + 2(\dot{\ell}_{2A} + \dot{\ell}_{2B}) \dot{\beta} \sin\beta + (\ell_{2A} + \ell_{2B}) \dot{\beta}^2 \cos\beta + \ell_3 \dot{\phi}^2 \sin\phi \\ \ell_{2B} - (\ell_{2B})_{\text{UNSATURATED}} \end{bmatrix}$$

## PART 4

For the final situation, both  $\ell_{2A}$  and  $\ell_{2B}$  are modeled as saturated. This gives the system three degrees-of-freedom. This third degree-of-freedom requires a third state variable so that the system can be solved. For this case, the third state variable is  $x$ , the displacement of the endmass. This makes the initial conditions for this system  $\theta, \dot{\theta}, \phi, \dot{\phi}, x$ , and  $\dot{x}$ .

The same initial equation which has been used for the past two situations will again be used in this one

$$\beta = \tan^{-1} \left[ \frac{L - \ell_1 \sin \theta - \ell_3 \sin \phi}{\ell_3 \cos \phi - \ell_1 \cos \theta} \right] \quad (\text{A4-1})$$

The next equation is derived from Equation (19) in the text to give

$$\ell_{2A} = \frac{x - \ell_1 \sin \theta}{\cos \beta} \quad (\text{A4-2})$$

The next equation is a copy of Equation (A3-2):

$$\ell_{2B} = \frac{\ell_3 \cos \phi - \ell_1 \cos \theta - \ell_{2A} \sin \beta}{\sin \beta} \quad (\text{A4-3})$$

The next three equations must be solved simultaneously. The three initial equations are Equation (20) from the text and Equations (A1-3) and (A1-4). Rather than having them solve by the computer every time, they were done by hand and simple equations used instead. These equations were

$$\dot{\beta} = \frac{1}{(\ell_{2A} + \ell_{2B}) \cos \beta} \left[ \ell_1 \dot{\theta} \sin \theta - \ell_3 \dot{\phi} \sin \phi + \sin \beta (\ell_1 \dot{\theta} \cos(\beta + \theta) + \ell_3 \dot{\phi} \cos(\beta - \phi)) \right] \quad (\text{A4-4})$$

$$\dot{\ell}_{2A} = \frac{1}{\cos \beta} \left[ \dot{x} - \ell_1 \dot{\theta} \cos \theta + \dot{\beta} (\ell_{2A} \sin \beta + d_1 \cos \beta + d_2 \sin \beta) \right] \quad (\text{A4-5})$$

$$\dot{\ell}_{2B} = -\ell_1 \dot{\theta} \cos(\beta + \phi) - \ell_3 \dot{\phi} \cos(\beta - \phi) - \dot{\ell}_{2A} \quad (\text{A4-6})$$

The next 10 equations must be solved simultaneously in order to give the rest of the information on the system. The matrices used are

$$[\tilde{A}] = \begin{bmatrix} \frac{1}{3}m_1\ell_1^2 & 0 & 0 & -\ell_1\cos\theta & \ell_1\sin\theta & 0 & 0 & 0 & 0 & 0 \\ 0 & \frac{1}{3}m_3\ell_3^2 & 0 & 0 & 0 & -\ell_3\cos\phi & \ell_3\sin\phi & 0 & 0 & 0 \\ -\ell_1\cos\theta & 0 & \ell_{2A}\sin\beta + d_1\cos\beta + d_2\sin\beta & -\frac{1}{m_2} & 0 & \frac{1}{m_2} & 0 & -\cos\beta & 0 & 1 \\ \ell_1\sin\theta & 0 & -(\ell_{2A}\cos\beta - d_1\sin\beta + d_2\cos\beta) & 0 & -\frac{1}{m_2} & 0 & -\frac{1}{m_2} & -\sin\beta & 0 & 0 \\ 0 & 0 & -I_2 & -(\ell_{2A}\sin\beta + d_1\cos\beta + d_2\sin\beta) & \ell_{2A}\cos\beta - d_1\sin\beta + d_2\cos\beta & -\ell_{2B}\sin\beta - d_1\cos\beta + d_2\sin\beta & -\ell_{2B}\cos\beta - d_1\sin\beta + d_2\cos\beta & 0 & 0 & 0 \\ -\ell_1\sin\theta & \ell_3\sin\phi & -(\ell_{2A} + \ell_{2B})\cos\beta & 0 & 0 & 0 & 0 & \sin\beta & \sin\beta & 0 \\ \ell_1\cos\theta & \ell_3\cos\phi & -(\ell_{2A} + \ell_{2B})\sin\beta & 0 & 0 & 0 & 0 & \cos\beta & \cos\beta & 0 \\ 0 & 0 & 0 & \frac{1}{\text{Stiff}}\cos\beta & \frac{1}{\text{Stiff}}\sin\beta & 0 & 0 & 0 & 0 & 0 \\ 0 & 0 & 0 & 0 & 0 & \frac{1}{\text{Stiff}}\cos\beta & -\frac{1}{\text{Stiff}}\sin\beta & 0 & 0 & 0 \\ 0 & 0 & 0 & -1 & 0 & 1 & 0 & 0 & 0 & -m_2 \end{bmatrix}$$

$$[\tilde{x}] = \begin{bmatrix} \ddot{\theta} \\ \ddot{\phi} \\ \ddot{\beta} \\ B_x \\ B_y \\ C_x \\ C_y \\ \ddot{\ell}_{2A} \\ \ddot{\ell}_{2B} \\ \ddot{x} \end{bmatrix}$$

$$[\tilde{c}] = \begin{bmatrix} -k_1\theta \\ -k_3\phi \\ -\ell_1\dot{\theta}^2\sin\theta - 2\dot{\ell}_{2A}\dot{\beta}\sin\beta - \dot{\beta}^2(\ell_{2A}\cos\beta - d_1\sin\beta + d_2\cos\beta) \\ -\ell_1\dot{\theta}^2\cos\theta + 2\dot{\ell}_{2A}\dot{\beta}\cos\beta - \dot{\beta}^2(\ell_{2A}\sin\beta + d_1\cos\beta + d_2\sin\beta) \\ 0 \\ \ell_1\dot{\theta}^2\cos\theta - 2(\dot{\ell}_{2A} + \dot{\ell}_{2B})\dot{\beta}\cos\beta + (\ell_{2A} + \ell_{2B})\dot{\beta}^2\sin\beta - \ell_3\dot{\phi}^2\cos\phi \\ \ell_1\dot{\theta}^2\sin\theta + 2(\dot{\ell}_{2A} + \dot{\ell}_{2B})\dot{\beta}\sin\beta + (\ell_{2A} + \ell_{2B})\dot{\beta}^2\cos\beta + \ell_3\dot{\phi}^2\sin\phi \\ \ell_{2A} - (\ell_{2A})_{\text{UNSATURATED}} \\ \ell_{2B} - (\ell_{2B})_{\text{UNSATURATED}} \\ 0 \end{bmatrix}$$



## APPENDIX B

## EQUATIONS FOR THE SPRING-DAMPER METHOD

The system which uses springs and dampers between the endmass and the ends of the beams has three degrees-of-freedom. This means that three state variables are required to describe the position of the system at any time. For this simulation, these variables are  $\theta$ , which describes the angular position of Beam 1;  $\phi$ , which describes the angular position of Beam 2; and  $x$ , which describes the linear position of the endmass. As state variables, these will be the variables which are integrated to give the initial conditions for the system, which will be  $\theta, \dot{\theta}, \phi, \dot{\phi}, x$ , and  $\dot{x}$ .

The equations as described here are the same as those in Part 4 of Appendix A. This is because both systems have three degrees-of-freedom and start from the same initial conditions. The equations will be listed here for the sake of completeness

$$\beta = \tan^{-1} \left[ \frac{L - \ell_1 \sin \theta - \ell_3 \sin \phi}{\ell_3 \cos \phi - \ell_1 \cos \theta} \right] \quad (\text{B-1})$$

$$\ell_{2A} = \frac{x - \ell_1 \sin \theta}{\cos \beta} \quad (\text{B-2})$$

$$\ell_{2B} = \frac{\ell_3 \cos \phi - \ell_1 \cos \theta - \ell_{2A} \sin \beta}{\sin \beta} \quad (\text{B-3})$$

$$\dot{\beta} = \frac{1}{(\ell_{2A} + \ell_{2B}) \cos \beta} \left[ \ell_1 \dot{\theta} \sin \theta - \ell_3 \dot{\phi} \sin \phi + \sin \beta (\ell_1 \dot{\theta} \cos(\beta + \theta) + \ell_3 \dot{\phi} \cos(\beta - \phi)) \right] \quad (\text{B-4})$$

$$\dot{\ell}_{2A} = \frac{1}{\cos \beta} \left[ \dot{x} - \ell_1 \dot{\theta} \cos \theta + \dot{\beta} (\ell_{2A} \sin \beta + d_1 \cos \beta + d_2 \sin \beta) \right] \quad (\text{B-5})$$

$$\dot{\ell}_{2B} = -\ell_1 \dot{\theta} \cos(\beta + \theta) - \ell_3 \dot{\phi} \cos(\beta - \phi) - \dot{\ell}_{2A} \quad (\text{B-6})$$

We find a difference in the simultaneous equations to be solved, though. Because there are no actuators, the equations which were formerly used for them in the system of equations will be replaced with equations describing the forces resulting from the spring and damper. These equations are of the form:

$$B_x \cos\beta + B_y \sin\beta = \text{DAMP}(\dot{x} - \ell_1 \dot{\theta}) + \text{STIFF}\left(x - \ell_1 \theta - (\ell_{2A})_{\text{Natural Length}}\right) \quad (\text{B-7})$$

$$C_x \cos\beta - C_y \sin\beta = \text{DAMP}(-\ell_3 \dot{\phi} - \dot{x}) + \text{STIFF}\left(L - \ell_3 \phi - x - (\ell_{2B})_{\text{Natural Length}}\right) \quad (\text{B-8})$$

where DAMP is the damping coefficient of the dampers between the beam and the endmass

STIFF is the stiffness of the spring between the beam and the endmass

$(\ell_{2X})_{\text{Natural Length}}$  is the natural length of the spring

This makes the variables in the system of equations

$$[\tilde{A}] = \begin{bmatrix} \frac{1}{3}m_1\ell_1^2 & 0 & 0 & -\ell_1\cos\theta & \ell_1\sin\theta & 0 & 0 & 0 & 0 & 0 \\ 0 & \frac{1}{3}m_3\ell_3^2 & 0 & 0 & 0 & -\ell_3\cos\phi & \ell_3\sin\phi & 0 & 0 & 0 \\ -\ell_1\cos\theta & 0 & \ell_{2A}\sin\beta + d_1\cos\beta + d_2\sin\beta & -\frac{1}{m_2} & 0 & \frac{1}{m_2} & 0 & -\cos\beta & 0 & 1 \\ \ell_1\sin\theta & 0 & -(\ell_{2A}\cos\beta - d_1\sin\beta + d_2\cos\beta) & 0 & -\frac{1}{m_2} & 0 & -\frac{1}{m_2} & -\sin\beta & 0 & 0 \\ 0 & 0 & -I_2 & -(\ell_{2A}\sin\beta + d_1\cos\beta + d_2\sin\beta) & \ell_{2A}\cos\beta - d_1\sin\beta + d_2\cos\beta & -\ell_{2B}\sin\beta - d_1\cos\beta + d_2\sin\beta & -\ell_{2B}\cos\beta - d_1\sin\beta + d_2\cos\beta & 0 & 0 & 0 \\ -\ell_1\sin\theta & \ell_3\sin\phi & -(\ell_{2A} + \ell_{2B})\cos\beta & 0 & 0 & 0 & 0 & \sin\beta & \sin\beta & 0 \\ \ell_1\cos\theta & \ell_3\cos\phi & -(\ell_{2A} + \ell_{2B})\sin\beta & 0 & 0 & 0 & 0 & \cos\beta & \cos\beta & 0 \\ 0 & 0 & 0 & \cos\beta & \sin\beta & 0 & 0 & 0 & 0 & 0 \\ 0 & 0 & 0 & 0 & 0 & \cos\beta & -\sin\beta & 0 & 0 & 0 \\ 0 & 0 & 0 & -1 & 0 & 1 & 0 & 0 & 0 & -m_2 \end{bmatrix}$$

$$[\tilde{x}] = \begin{bmatrix} \ddot{\theta} \\ \ddot{\phi} \\ \ddot{\beta} \\ B_x \\ B_y \\ C_x \\ C_y \\ \ddot{\ell}_{2A} \\ \ddot{\ell}_{2B} \\ \ddot{x} \end{bmatrix}$$

$$[\tilde{C}] = \begin{bmatrix} -k_1\theta \\ -k_3\phi \\ -\ell_1\dot{\theta}^2\sin\theta - 2\dot{\ell}_{2A}\dot{\beta}\sin\beta - \dot{\beta}^2(\ell_{2A}\cos\beta - d_1\sin\beta + d_2\cos\beta) \\ -\ell_1\dot{\theta}^2\cos\theta + 2\dot{\ell}_{2A}\dot{\beta}\cos\beta - \dot{\beta}^2(\ell_{2A}\sin\beta + d_1\cos\beta + d_2\sin\beta) \\ 0 \\ \ell_1\dot{\theta}^2\cos\theta - 2(\dot{\ell}_{2A} + \dot{\ell}_{2B})\dot{\beta}\cos\beta + (\ell_{2A} + \ell_{2B})\dot{\beta}^2\sin\beta - \ell_3\dot{\phi}^2\cos\phi \\ \ell_1\dot{\theta}^2\sin\theta + 2(\dot{\ell}_{2A} + \dot{\ell}_{2B})\dot{\beta}\sin\beta + (\ell_{2A} + \ell_{2B})\dot{\beta}^2\cos\beta + \ell_3\dot{\phi}^2\sin\phi \\ \text{DAMP}(\dot{x} - \ell_1\dot{\theta}) + \text{STIFF}\left(x - \ell_1\theta - (\ell_{2A})_{\text{Natural Length}}\right) \\ \text{DAMP}(-\ell_3\dot{\phi} - \dot{x}) + \text{STIFF}\left(L - \ell_3\phi - x - (\ell_{2B})_{\text{Natural Length}}\right) \\ 0 \end{bmatrix}$$